2009 IEEE/ASME International Conference on Advanced Intelligent Mechatronics
Suntec Convention and Exhibition Center
Singapore, July 14-17, 2009

Grasp Synthesis Based on Tactile Sensation in Robot Manipulation of Arbitrary Located Object

Hanafiah Yussof, *Member, IEEE*, Jiro Wada, Masahiro Ohka

***Abstract*—This paper analyzes grasp synthesis in multi-fingered robot arm equipped with a tactile sensor to handle objects located at arbitrary positions. We developed an 11-dof multi-fingered arm and a novel optical three-axis tactile sensor system based on an optical waveguide transduction method. The tactile sensor can simultaneously acquire normal and shearing forces. We analyzed normal and shear force distribution to grasp real object. The slippage direction acquired from the shear force data was used to control arm movements in the incipient grasp and release motion. Normal force is used to distinguish object stiffness and to generate optimum grasp pressure. The analysis results are compiled in a control algorithm inside the robot control system. The algorithm was evaluated in experiments with real objects, and the results revealed good performance of the robot arm when handling arbitrary located objects.**

I. Introduction

RECENTLY interest has been growing in dexterous robot manipulation using tactile sensors. Tactile sensors offer great potential for improving the grasp synthesis in robot manipulation due to their extreme sensitivity and capability of measuring normal and shearing forces. In addition, material and stability recognition capabilities are advantages of a robotic arm equipped with a tactile sensor.

Object grasping is a typical human ability that is widely studied from both biological and engineering points of view. The problem of synthesizing the control of real-time grasp is an essential component of dexterous manipulation. To address this problem, Dubey [1] proposed a controller based on fuzzy logic that can perform the optimal grasp of objects without knowing their mass and frictional properties. Tomovic [2] analyzed grasping tasks as performed by human beings that indicated geometric modeling in target identification to complete the grasping task. In addition, Lim [3] proposed a real-time grasp planning architecture in multi-fingered hands to find grasp configurations that satisfy force-closure condition of arbitrary shaped objects.

Manipulation of objects located at an arbitrary position is also an essential component of dexterous manipulation task,

Hanafiah Yussof is with the Graduate School of Information Science, Nagoya University, Nagoya, Japan, and Faculty of Mechanical Engineering, Universiti Teknologi MARA, Malaysia. (e-mail: hanafiah@nuem.nagoya-u.ac.jp). Jiro Wada is with the Graduate School of Engineering, Nagoya University, Nagoya, Japan (e-mail: wada@nuem.nagoya-u.ac.jp). Masahiro Ohka is with the Graduate School of Information Science, Nagoya University, Furo-cho Chikusa-ku Nagoya 464-8601 Japan (phone: +81-52-789-4251; e-mail:: ohka@is.nagoya-u.ac.jp)

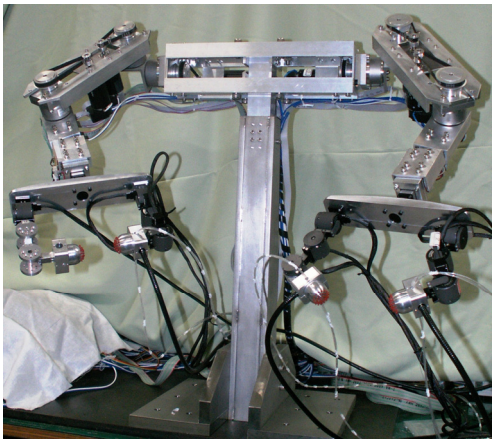

Fig. 1. Two multi-fingered robot arms equipped with optical three-axis tactile sensors at fingertips.

especially for robots that share workspace with humans. Several projects are focusing on these issues. For example, the ARMAR project, which is investigating manipulation in human environments, has shown results including the bimanual opening of a jar [4]. In addition, many groups are researching autonomous mobile manipulation in human environments [5][6], and robot manipulation for human-robot interaction using humanoid robots [7][8] that included the handling and transferring of objects between a humanoid and human. However, most of these projects have yet to consider tactile sensation for grasp synthesis in detail, whereby active visual perception is the main sensing modality used to recognize object and control grasping motions. Obviously, robots must be able to perform human-like grasp based on tactile sensation so that they can assist humans and work effectively in built-for-human environments.

In this research, we developed two units of 11-dofs multi-fingered robot arms to improve their maneuvering when handling real objects, as shown in Fig. 1. We present grasp synthesis analysis of arbitrary located objects based on tactile sensing. We developed a novel tactile sensor system to mount on each fingertip of the robot arm to realize tactile sensation. The tactile sensor is based on an optical waveguide transduction method and applies image processing techniques. Such a sensing principle is expected to provide better sensing accuracy to realize contact phenomena by acquiring the three axial directions of the forces, so that normal and shear forces can be measured simultaneously.

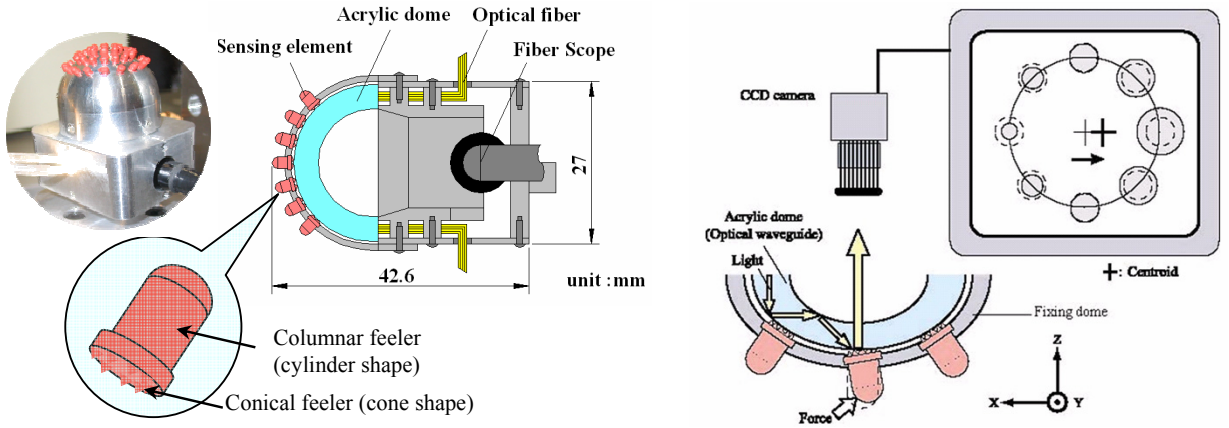

Fig. 2. Structure of optical three-axis tactile sensor and its sensing principles.

II. Hardware Structure and Sensing Principles of Optical Three-Axis Tactile Sensor

In this research, we analyzed grasp synthesis in robot manipulation by acquiring tactile sensing information using a multi-fingered robot arm equipped with an optical three-axis tactile sensor that is based on the principle of an optical waveguide-type tactile sensor. Fig. 2 shows the structure and the sensing principle of the tactile sensor system. The tactile sensor is designed in a hemispherical dome shape that consists of an array of sensing elements. This shape mimics the structure of human fingertips for easy compliance with various shapes of objects.

The novel hardware consists of an acrylic hemispherical dome, an array of 41 pieces of sensing elements made from silicon rubber, a light source, an optical fiber scope, and a CCD camera. The optical fiber-scope is connected to the CCD camera to acquire the images of sensing elements touching the acrylic dome inside the sensor. The silicone rubber sensing element is comprised of one columnar feeler and eight conical feelers that remain in contact with the acrylic surface. The light emitted from the light source is directed towards the edge of the hemispherical acrylic dome through optical fibers. When an object contacts the columnar feelers, resulting in contact pressure, the feelers collapse. At the points where the conical feelers collapse, light is diffusely reflected out of the reverse surface of the acrylic surface because the rubber has a higher reflective index. The contact phenomena, which consist of bright spots caused by the collapse of the feelers, are observed as image data, retrieved by the optical fiber scope connected to the CCD camera, and transmitted to the computer.

In the shearing force detection, when the tangential force is applied to the sensing element, it collapses based on the applied load direction. At the same time, the centroid point of the bright spot is also shifted. Therefore, the shearing force can be calculated based on the horizontal displacement of this centroid point.

In the measurement process, the normal forces of the F_x, F_y and F_z values are calculated using integrated gray-scale value G, while the shearing force is based on horizontal center point displacement. The displacement of gray-scale distribution $\boldsymbol{u}$ is defined in (1), where $\boldsymbol{i}$ and $\boldsymbol{j}$ are the orthogonal base vectors of the x- and y-axes of a Cartesian coordinate, respectively. This equation is based on calibration experiments, and material functions are initially identified with piecewise approximate curves [9]. Consequently, each force component is defined in (2):

$$\boldsymbol{u} = u_x\boldsymbol{i} + u_y\boldsymbol{j} \tag{1}$$

$$F_x = f(u_x),\ F_y = f(u_y),\ F_z = g(G). \tag{2}$$

The integrated gray-scale value of contact area $g(x,y)$ is proportional with contact force $p(x,y)$, as shown in (3):

$$p(x,y) = C_v \triangle g(x,y). \tag{3}$$

Here, C_v is a transformation coefficient, and $\triangle g(x,y)$ is increment of the integrated gray-scale value. Based on this relationship, we define the normal force from the gray-scale distribution of the contact area. The measurement of contact force P is defined by the following integration, where S is size of the gray-scale measurement area.

$$P = \int_S p(x,y)dS\ . \tag{4}$$

Here, when (3) is applied to (4), we can define measurement of contact force P as following Eq. (5):

$$P = C_v \int_S \Delta g(x,y)dS\ . \tag{5}$$

Next, we calculate the centroid position, which is measured based on the center point of the bright spots area that equals to the center position of the integrated gray-scale measurement area. When tangential force is applied to the sensor element, the conical feeler`s contact area at sensing element with the acryl surface is shifted horizontally. To define the shearing force, we measure the horizontal centroid point displacement at the x and y axes.

First, by applying the increment of integrated gray-scale value $\triangle g(x,y)$, the centroid positions at the *xy*-axes, which are described as x_G and y_G are defined within the measurement area of the integrated gray-scale value, as shown in Eqs. (6) and (7), respectively:

$$x_G = \frac{\int_S \Delta g(x,y) x dS}{\int_S \Delta g(x,y) dS} \tag{6}$$

$$y_G = \frac{\int_S \Delta g(x,y) y dS}{\int_S \Delta g(x,y) dS}. \tag{7}$$

Based on the above equations, the displacement of the centroid point at the *xy*-axes in time *t* is defined as follows:

$$dx_G^{(t)} = x_G^{(t)} - x_G^{(t-1)} \tag{8}$$

$$dy_G^{(t)} = y_G^{(t)} - y_G^{(t-1)}. \tag{9}$$

III. Grasp Synthesis Analysis

In this research, we analyze the grasp synthesis of robotic fingers that handle an object located at an arbitrary position. The analysis is based on normal and shearing forces acquired by tactile sensors.

A. Analysis of Normal Force Distribution

We conducted a series of experiments using the two robotic fingers to grasp real objects to clarify normal force distribution of our tactile sensor. The objects were a cube-sized aluminum block and a paper box. The experiment conditions are shown in Fig. 3; the robot fingers grasped the object to lift it up to the *z*-axis direction. Fig. 4 shows the normal force distributions of the sensing elements in both experiments.

In the experiment with an aluminum block, as shown in Fig. 4 (top), the normal force was increased drastically in incipient grasp due to the object's hard surface. At this moment, the finger control system recognized the incipient grasp and lifted the object up while maintaining grasp pressure on it. In the experiment with the paper box, as shown in Fig. 6 (bottom), the increment of the normal force is small due to the object's soft surface. However, since the response of the normal force can still be detected, the finger control system recognized the incipient grasp and then lifted the object.

From both experiments results, we conclude that it is possible to estimate object stiffness as indicated in the normal force distribution data. The methodology measures the increment of normal force data in a specified progress time so that it can be used to control the grasp pressure by refining the re-push velocity on the object.

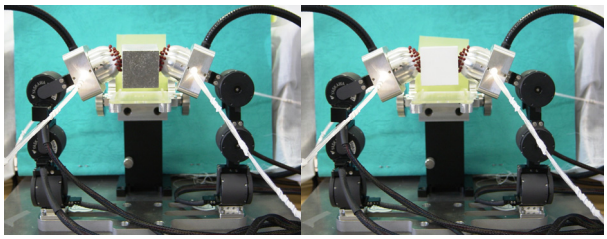

Fig. 3. Robot fingers grasp and lift aluminum block and paper box.

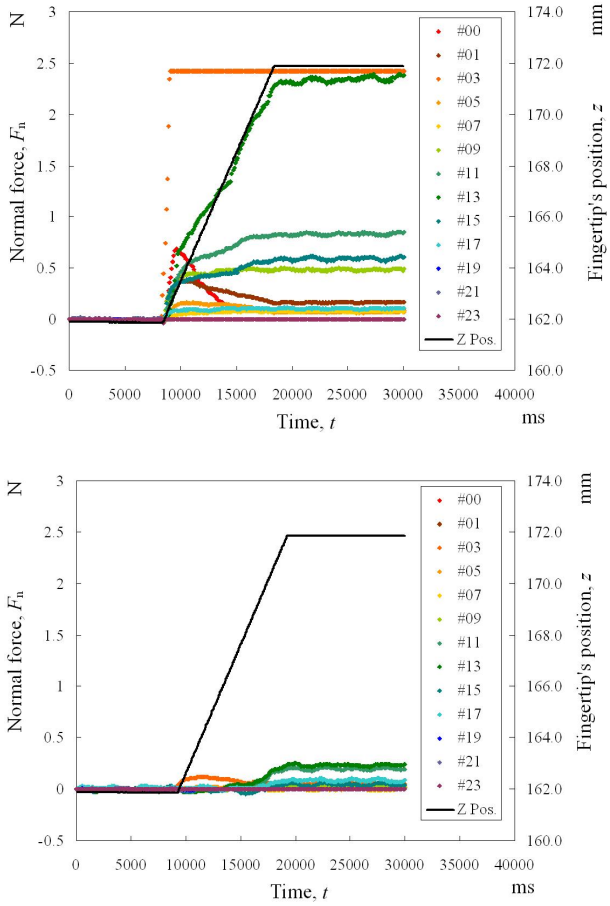

Fig. 4. Fingertip position and normal force distribution at left finger in experiments with aluminum block (top) and paper box (bottom).

B. Analysis of Shear Force Distribution

In the handling tasks of an arbitrary located object, slippage which occurred during the incipient grasp normally reflects the object's weight resistance. During the release motion, slippage that occurs is the result of the object contacting the ground surface. In this situation, without proper control of the robot arm, the possibility is high that the robot fingers will over-push toward the object during incipient grasp and towards the ground during release motion. Therefore, to avoid such problems that can damage the object or the tactile sensor, shear force characteristics and distribution must be analyzed during incipient grasp and release motion.

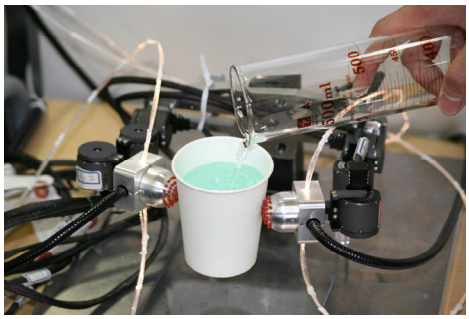

Fig. 5. Experiment of sudden weight change using robot fingers.

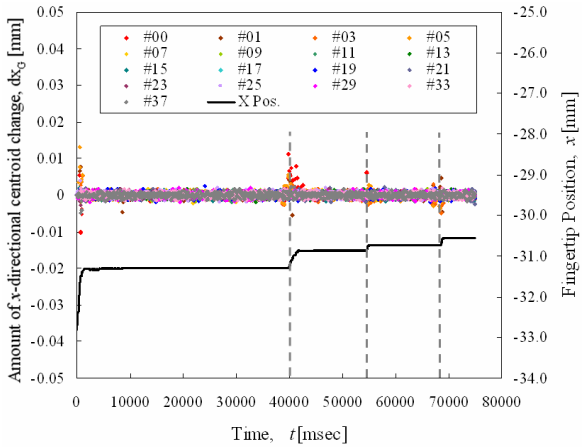

Fig. 6. Shear force data and right fingertip's position at *x*-axis in sudden weight change experiment.

First, we analyzed the shear force response in the optical three-axis tactile sensor. We conducted experiments to clarify the tactile sensor response against a sudden change of object weight using two robot fingers mounted on a test jig as shown in Fig. 5, where the finger orientation is about horizontal with the table surface. The optical three-axis tactile sensors were mounted on both fingertips. The object was an empty paper cup that weighed about 4 grams. Motion planning was designed so that both fingers could move along the *x*-axis direction to grip the cup, lifting it along the *y*-axis direction within 80 sec of the progress time. Next, at 40 sec we poured 60 ml of water into the cup, and then after 55 sec we poured another 30 ml, and finally another 20 ml after about 70 sec.

The fingertip movements and the detected shear force data of both fingers are compiled in graph. In Fig. 6, the movement of the right fingertip can be observed at the *x*-axis against the detected shear force. In this experiment, when water was poured into the cup, slippage was detected by tactile sensors as shown in centroid changes at the *x*-directional of the sensor elements. The finger system recognizes the slippage and responds quickly by adjusting the fingertip position to tighten the grip so that the paper cup will not slip. The robot fingers managed to react to the object's sudden weight change of object weight by acquisition of shear force data from the tactile sensor.

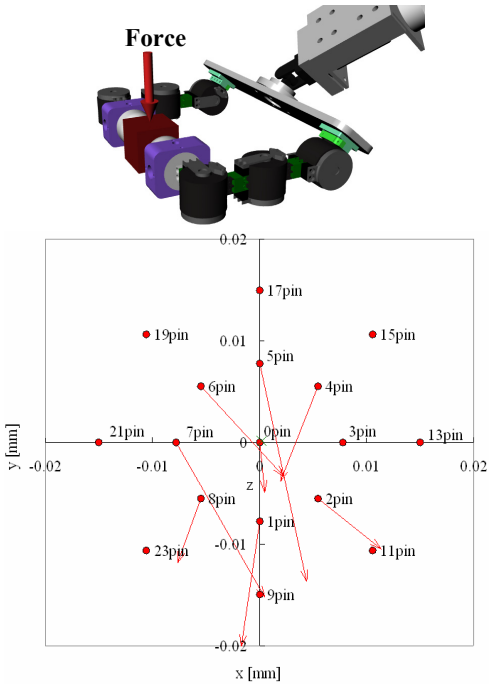

Fig. 7. Centroid displacement of tactile sensor elements in analysis of shear force and slippage direction when force applied at object's center.

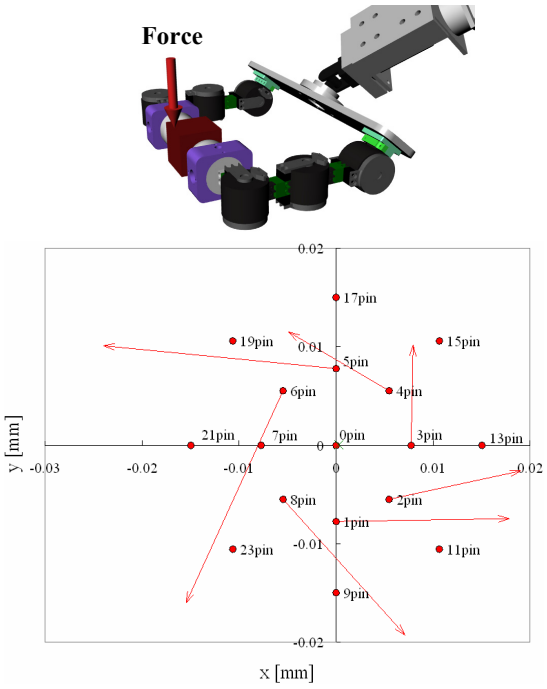

Fig. 8. Centroid displacement of tactile sensor elements in analysis of shear force and slippage direction when force applied at object's edge.

From these experimental results, we conclude that the optical three-axis tactile sensor used in this research can detect sudden slippage sensations. Therefore it is suitable to classify incipient grasp and release motion while arbitrary located objects are being handled.

Second, since clarifying the shear force characteristics and distribution is important in both the incipient grasp and release motion, we conducted a simple experiment in which the robot finger held a cube-shaped object as illustrated in Fig. 7 and 8. First we applied force to the center of the object, as shown in Fig. 7, and then at its edge as shown in Fig. 8, which caused the object to slightly rotate. We defined the shear force characteristics and distribution by calculating the centroid point displacement of the sensing elements, as indicated in the graphs for both experiments.

The graphs in Figs. 7 and 8 show the directions of the centroid displacements of the related tactile sensor elements are toward the applied force direction. In Fig. 8, the directions of the centroid displacement for the tactile sensor elements are based on to the object's rotation direction.

From both experiment results, we conclude that the shear force direction reflects the applied force direction. Therefore slippage direction can be used as a control parameter in the robot arm control system to distinguish incipient grasp and release motion. In addition, the optical three-axis tactile sensor is highly sensitive for detecting shear force that enables the robot arm to precisely control the finger motion during incipient grasp and release motion.

IV. Verification Experiment

In our previous works [10][11], we defined suitable tactile sensing-based control parameters in our robot arm control system using the optical three-axis tactile sensor. The parameters are shown in Table 1. Based on these parameters, we proposed a control algorithm to classify object stiffness and generate suitable grasp motion.

We classified objects into three classifications to control the optimum grasping pressure: soft, medium, and hard. These classifications are used to select the velocity ratio for the velocity of re-push motion v_p. The threshold of normal forces F_1 and F_2 functioned to control finger movement during grasping and manipulating objects.

During the re-push motion, the selection of the thresholds of normal forces F_1 and F_2 and the re-push velocity are decided based on the object hardness classification. Based on the normal force thresholds, the velocity ratio was defines to re-push toward the object and to decide to stop the motion.

In the control algorithm, first the control system sees the threshold of centroid change dr before performing stiffness distinction using the increment of normal force ΔF. Then the fingers reinforce the grasping pressure to re-push the object based on the velocity ratio. Regarding the threshold of normal force, if the object was detected as soft, the finger no longer re-pushes the object when the detected normal force exceeds F_1. Meanwhile, F_2 is used for emergency stops so that the finger will not over-push the object.

TABLE I. Control Parameters of Object Manipulation

Category		Parameter
Sampling interval	Sensor	100 ms
	Finger	25 ms
Threshold of normal force	F_1	0.5 N
	F_2	1.8 N
Threshold of shearing force	dr	0.004 mm
Velocity of re-push	v_p	2 mm/s
Velocity ratio	(Soft, medium, hard)	(0.25,1.00,1.25)
Increment of normal force	ΔF	soft< 0.08 N <hard
Progress time	Δt	0.1 s

As mentioned in Section *III*, the slippage direction is based on the applied force direction. In our robot control system, we fixed the slippage direction to classify the incipient grasp and set the timing of the release motion. When the distribution of the shear force direction is downward (positive side), the robot control system classifies the motion as incipient grasp. If the distribution of the shear force direction is upward (negative side), the control system automatically realizes that the object is contacting the ground. Therefore, the arm will not move any further, and the fingers gently release the object.

We conducted an object transferring motion experiment to verify the performance of the multi-fingered robot arm when handling a cube-shaped wood block object located at an arbitrary position. The optical three-axis tactile sensors are mounted on the fingertips of both fingers. Fig. 9 shows photographs of the experimental conditions. The robot arm grasped, moved and released the object. Fig. 10 shows the relationship at the left finger between the fingertip positions and the shear force distribution which were calculated from the arm's global coordinates.

In this experiment, the fingers start to grasp and release the object when the slippage value exceeds the fixed threshold value. This can be observed in the graph at the changes of fingertip movement that correlate with the detection of the shear force distribution. Related with the shear force direction, during incipient grasp, both positive and negative directions can be observed. This is caused by the rotation of the object due to the weight to adjust its position. At this moment, the finger control system managed to perform grasp and release motions since the first detections of slippage are at the positive side.

Meanwhile, during the release motion, both positive and negative directions can also be observed due to the object rotation when the object touches the ground. However, the first shear force was detected at the negative side, as shown on the right in Fig. 10. The robot arm knows that the object is touching the ground and stops further movement toward it. Then the fingers slowly release the object.

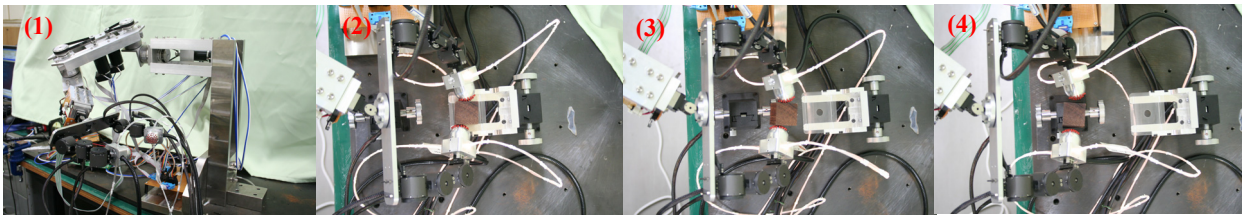

Fig. 9. Sequential photographs in object transferring experiment using wood block.

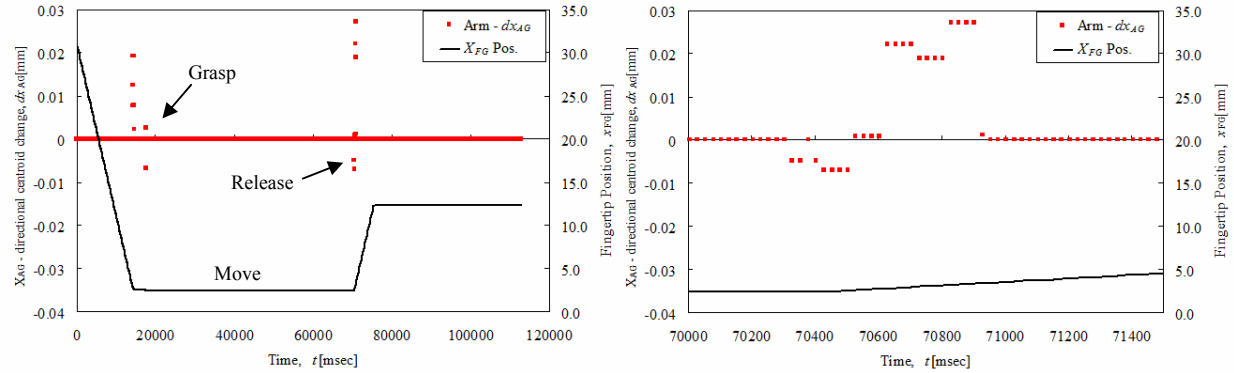

Fig. 10. Object transfer experiment data of left finger using wood block. Relationship between *x*-directional centroid displacement calculated about *x*-axis arm`s global coordinate, and *x*-directional fingertip position. *(Left)* For all motions. *(Right)* During release motion.

V. Conclusions

Tactile sensors have great potential for improving grasp synthesis in robot manipulation. The problem of synthesizing the control of real-time grasp is an essential component of dexterous manipulation. Furthermore, handling objects located at arbitrary positions based on tactile sensation is a new challenge in robot manipulation.

In this report, we presented an analysis of grasp synthesis based on tactile sensation for grasping and handling an object located at an arbitrary position. The analysis was conducted using a multi-fingered robot arm equipped with an optical three-axis tactile sensor. To manipulate an arbitrary located object, we conducted an analysis of normal force and shear force distribution. Furthermore we analyzed the slippage direction to distinguish grasp synthesis in the incipient grasp and release motion. We proposed a control algorithm based on tactile-slippage sensation to define object stiffness and to generate suitable grasp pressure. The analysis results were applied in the control algorithm to define suitable timing to lift and release an object.

Finally, the proposed control algorithm's performance was experimentally evaluated using real objects. The experimental results revealed good performance for robot fingers in defining optimum grasp pressure and in autonomously controlling the grasp and release motions of the object at an arbitrary position.

Acknowledgment

A part of this study was supported by fiscal 2008-2010 Grant-in-Research by The Japan Society for the Promotion of Science (JSPS) no. P 08062.

References

[1] V. N. Dubey, R. M. Crowder and P. H. Chappell, "Optimal object grasp using tactile sensors and fuzzy logic," *Robotica*, vol. 17, issue 6, Nov. 1999, pp. 685-693.

[2] R. Tomovic, G. Bekey and W. Karplus, "A strategy for grasp synthesis with multifingered robot hands," *Proceeding of ICRA '87*, Vol.4, 1987, pp. 83-89.

[3] M. Lim, S. Oh, J. Son, B. You and K. Kim, "A human-like real-time grasp synthesis method for humanoid robot hands," *Journal of Robotics and Autonomous System*, Vol. 30, 2000, pp. 261-271.

[4] R. Zollner, T. Asfour & R. Dillmann, "Programming by demonstration: dual-arm manipulation tasks for humanoid robots," in *Proc. of 2004 IEEE/RSJ International Conference on Intelligent Robots and Systems (IROS 2004)*. Vol. 1, pp. 479 – 484, 2004.

[5] O. Khatib, K. Yokoi and A. Casal, "Robots in human environments: Basic autonomous capabilities," *International Journal of Robotics Research*, Vol. 18, No. 7, pp. 684-696, 1999.

[6] S. Caselli, E. Fantini, F. Monica, P. Occhi and M. Reggiani, "Toward a mobile manipulator service robot for human assistance," in *Proc. of the 1st Robocare Workshop*, Roma, Italy, 2003.

[7] A. Edsinger and C. Kemp, "Manipulation in human environments," in *Proc. Int. Conf. on Humanoid Robotics (Humanoids06)*, Italy. 2006

[8] N. Sian, K. Yokoi, Y. Kawai, and K. Murayama, "Operating humanoid robots in human environments," in *Proc. of Robotic, Science and Systems: Workshop on Manipulation for Human Environments*, Philadelphia, USA, 2006.

[9] M. Ohka, H. Kobayashi and Y. Mitsuya, "Sensing precision of an optical three-axis tactile sensor for a robotic finger," in *Proc. 15th RO-MAN06*, Sept. 2006, Hatfield, United Kingdom, pp. 220-225.

[10] H. Yussof, M. Ohka, A. R. Omar, and M. A. Ayub, "Determination of Object Stiffness Control Parameters in Robot Manipulation Using a Prototype Optical Three-Axis Tactile Sensor," in *Proceedings of The 7th IEEE International Conference on Sensors (SENSORS2008)*, pp. 992-995, Lecce, Italy, Oct. 26-29, 2008.

[11] H. Yussof, M. Ohka, J. Takata, Y. Nasu and M. Yamano, "Low Force Control Scheme for Object Hardness Distinction in Robot Manipulation Based on Tactile Sensing," in *Proceedings of The 2008 IEEE International Conference on Robotics and Automation (ICRA2008)*, pp. 3443-3448, Pasadena, CA, USA, May 19-23, 2008.